Mathematical Oncology: Using Mathematics to Enable Cancer Discoveries

Trachette Jackson, Natalia Komarova, and Kristin Swanson

Abstract. Mathematical and computational modeling approaches have been applied to every aspect of tumor growth from mutation acquisition and tumorigenesis to metastasis and treatment response. In this article, we discuss some of the current mathematical trends in the field and the exciting applications and challenges that lie ahead. In particular, we focus on mathematical approaches that are able to address critical questions associated with tumor initiation; angiogenesis and vascular tumor growth; and the new frontier of computer-aided, patient-specific cancer evaluation and treatment.

1. INTRODUCTION. Cancer is the collective name given to an entire class of diseases characterized by rapid, uncontrolled cell growth. There are over 200 different types of cancer, each classified by the type of cell that is initially affected. Normally, our bodies form new cells only as we need them. However, when cells acquire mutations that disrupt the tightly controlled processes of cell division and death, a self-sustaining wave of cellular multiplication can occur and result in the formation of a tumor. To ensure its continued growth, a tumor must acquire a continuous supply of nutrients and the ability to export metabolic waste. It does this by recruiting new blood vessels from the nearby existing vasculature, a process known as tumor-induced angiogenesis. Angiogenesis provides the necessary blood supply for the growth of solid tumors beyond a few millimeters in diameter. Tumors that remain relatively localized in the tissue of origin and demonstrate limited growth are generally considered to be benign. More dangerous malignant tumors form when cancer cells invade and destroy healthy tissue and metastasize. Tumor cells using the blood or lymphatic system as a highway to move throughout the body and form new malignant masses characterize metastasis. See Figure 1 for a schematic representation of tumor progression, including mutation acquisition, blood vessel formation, vascular tumor growth, invasion, and metastasis.

Author Proof

It is estimated that in our country alone over 4500 new cancer cases are diagnosed every day and that over half a million Americans will die from cancer this year [**63**]. Due to the inherent complexity of the many interconnected physiological processes involved in tumor initiation and progression, on both the cellular and tissue levels, conventional experimental approaches alone often fail to provide complete understanding of cancer. Given the multiscaled pathophysiology involved, it is becoming more and more important for cancer research to make use of a cross-disciplinary, complex, systems science approach in which mathematical models play a central role.

Existing mathematical models in oncology have employed a number of methodologies: continuous approaches, wherein molecules, cells, and/or tissue components are assumed to have a continuous distribution; stochastic approaches that estimate probability distributions of potential cellular outcomes; discrete or hybrid models, in which cells are modeled as individual agents and diffusible chemicals are modeled as a continuum; and cell-based formulations that explicitly incorporate different properties of AQ1

http://dx.doi.org/10.4169/amer.math.monthly.121.09.000
MSC: Primary 92B05

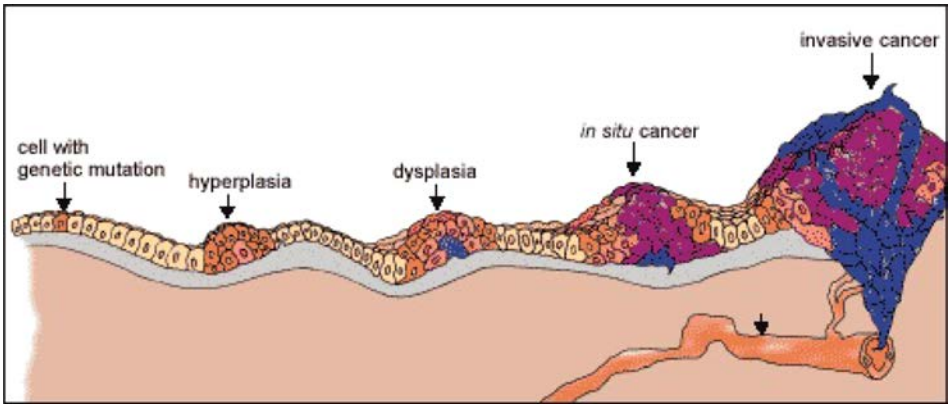

Figure 1. A schematic of tumor initiation, angiogenesis, and invasion taken from http://www.ndhealthfacts.org/wiki/Oncology. The figure shows the initiating genetic mutation, abnormal cellular growth (hyperplasia and dysplasia), early tumor growth in the absence of invasion (in situ cancer), followed by angiogenesis, invasion, and metastasis.

individual cells in order to predict collective tissue behavior. The vast amount of clinical data and basic science research produced today is allowing for the development of new mathematical models that incorporate one or more of these approaches and that have unprecedented depth, accuracy, and predictive power. Such models have the potential to facilitate a deeper understanding of the cellular and molecular interactions associated with tumor initiation, progression, and treatment. This article highlights several mathematical modeling approaches in order to illustrate some of the emerging trends in the field of mathematical oncology. In keeping with the natural progression of tumorigenesis described above (initiation, angiogenesis, vascular tumor growth), in the opening sections we feature mathematical approaches that address one of the oldest and most important questions in oncology: How do tumors arise and what cellular and molecular factors are most influential for cellular transformation and tumor initiation? Once a tumor has formed, it must acquire a vascular supply. We therefore continue on to spotlight how multiscale modeling can aid in understanding the critical steps that follow tumor initiation, namely, tumor angiogenesis and vascular tumor growth. Vascular tumors in individual patients are as different as we are as people; what works to treat one person's disease may completely fail in another patient. Therefore, in closing we showcase promising successes in the newest frontier of cancer therapy: patient-specific mathematical neuro-oncology.

Author Proof

2. ADVANCES IN MODELING TUMOR INITIATION AND CANCER STEM CELLS.

The question of the origins of cancer is among the most important in our understanding of the disease. There is no universal answer to this question, as different cancers are initiated by different mechanisms. There are, however, certain patterns that can be recognized. Among the most prominent ones are cancer initiation via (1) an activation of oncogenes and (2) an inactivation of tumor suppressor genes and also the recently described universal sequence of events for stem-cell-driven cancers. Here we study these patterns by means of stochastic and deterministic evolutionary models.

Concepts. Some mutations directly lead to the generation of advantageous mutants. This is characteristic of the *gain-of-function* mutations (see, e.g., [**66**]) that activate *oncogenes*, which are modified genes that increase the malignancy of a tumor cell.

A *loss-of-function* mutation results in a gene product having less or no function. Two independent loss-of-function mutations are necessary to inactivate a gene because, after the first mutation, the second copy of the gene is still active. In the context of cancer, the loss-of-function mechanism is involved in the inactivation of tumor suppressor genes, which are protective genes that normally limit the growth of tumors.

The Moran process is a useful tool to study oncogenesis, including oncogenes and tumor suppressor genes, both analytically and numerically [**43**]. This stochastic, cell-based model describes cellular turnover in constant populations. An elementary update consists of a cell death (whereby the cell is chosen for death randomly with a uniform probability), followed immediately by a cell division. To include competition, each cell is equipped with a fitness parameter, and divisions happen with the probability proportional to the cell fitness. Upon division, with a small fixed probability, a cell can mutate, such that one of the daughter cells belongs to a different type (and thus may have a different fitness). The number of elementary updates per time unit is proportional to the total population size. Figure 2 shows the basic Moran process, which we call the mass-action (complete mixing) model (a), as well as a spatial process, where reproduction happens in a cell's neighborhood (b), and a hierarchical process, which keeps track of stem cells and differentiated cells (c). The analytical results below pertain to the mass-action process [**30, 47**], and generalizations for the spatial [**16, 17, 27, 31**] and hierarchical [**28, 32, 59**] processes are available.

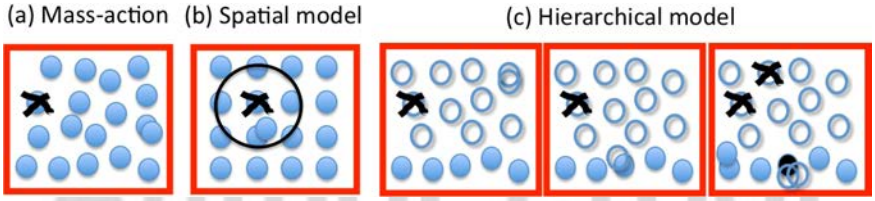

Author Proof

Figure 2. A schematic of one update of the Moran process (a) and two of its generalizations (b,c). (a) A mass-action process, where the probabilities of divisions and deaths are independent of spatial locations; (b) spatial Moran process in 2D; (c) the hierarchical model. Filled circles represent stem cells and empty circles differentiated cells. Following a differentiated cell death, a differentiated cell divides (left), a stem cell divides asymmetrically (middle), or two differentiated cell death events are balanced by two symmetric divisions of stem cells, one proliferation event and one differentiation event (right).

Dynamics of gain- and loss-of-function mutations. Mathematical tools enable us to gain analytical understanding of the complex dynamics of gain- and loss-of-function mutations. Let us first study the behavior of one-hit mutants (cells of type "B") that originate from the wild-type cells (type "A") with the mutation rate u_1, in a population of size N. We denote the relative fitness of the mutants as r; type "B" cells can be classified as negatively selected, positively selected, or neutral mutants; see Table 1. There are two very different dynamical regimes that are observed in this model depending on the parameters:

- **The two-state dynamics**, Figure 3(a). For small populations (conditions in Table 1), the system can be approximately described by (continuous time) stochastic transitions between two homogeneous states: the All-A state and the All-B state. The probability to find the system in a mixed state containing both types of cells is relatively low.
- **Nearly-deterministic dynamics**, Figure 3(b). For large populations, new mutants are produced frequently, and accumulate in a nearly deterministic fashion. In this

Table 1. Gain-of-function: definitions and conditions.

Types of mutant	definitions	conditions for the two-state process
Disadvantageous	$r < 1, \lvert 1-r\rvert \gg 1/N$	$u_1 N \ll r^{-(N-1)}$
Neutral	$\lvert 1-r\rvert \ll 1/N$	$u_1 N \ll 1$
Advantageous	$r > 1, \lvert 1-r\rvert \gg 1/N$	$u_1 N \ll r$

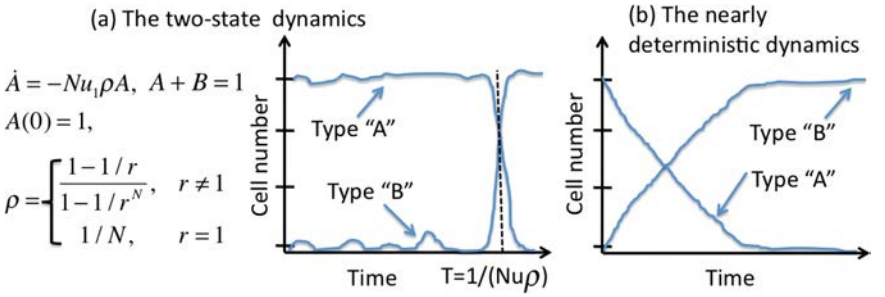

Figure 3. Gain-of-function: a schematic of the two types of behavior [**77**]. (a) A jump between the all-"A" and the all-"B" states (well approximated by the Markovian jump presented as the ODE on the left). (b) The nearly deterministic rise of mutants in the case of neutral or advantageous mutants. Disadvantageous mutants do not reach fixation but are maintained at a selection-mutation balance. ρ is the probability of fixation of type "B" starting from one cell.

regime, neutral mutants' dynamics will resemble the behavior of advantageous mutants because, in the absence of back-mutations, they will constantly grow in abundance.

To describe the dynamics of loss-of-function mutations, we modify the Moran process to include mutations from B to C with rate u_2. Type C (double-hit) mutants are assumed to be highly advantageous: Once this type is generated, it will invade the population with a high probability. Depending on the parameters, the dynamics of mutants can be classified into three distinct regimes.

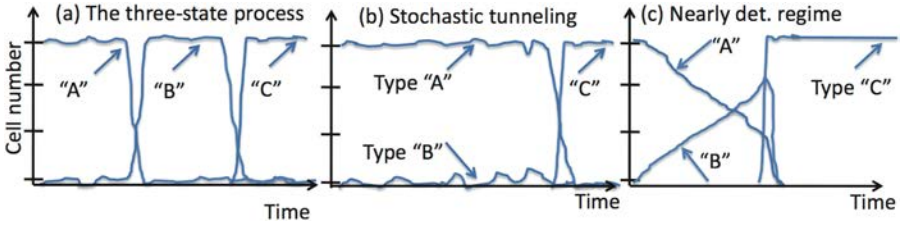

Figure 4. Loss-of-function: the three possible processes of two-hit mutant creation [**77**]. (a) The three-state process. (b) Stochastic tunneling. (c) Nearly deterministic process.

- **The three-state process**, Figure 4(a), is similar to the two-state process of Figure 3(a) and is observed for relatively small populations (Table 2). The system is accurately approximated by Markovian jumps between the All-A, All-B, and C states, with $A+B+C=1$: $\dot{A} = -Nu_1\rho A$, $\dot{B} = Nu_1\rho A - Nu_2 B$, $A(0)=1$, $B(0)=0$.
- **Stochastic tunneling**, Figure 4(b), is the processes where the system goes from the All-A state to the C state, skipping the intermediate fixation of type B. The concept of stochastic tunneling was introduced by [**30, 47**]. With R the constant tunneling rate, we can approximate the dynamics as $\dot{A} = -Nu_1 RA$, $A(0)=1$.

Author Proof

Table 2. Loss-of-function: definitions and conditions.

Type of mutant	definition	condition for the three-state process
Disadvantageous	$r < 1, \lvert 1-r\rvert \gg 1/N$	$N\lvert \ln r\rvert \ll \ln\left(\frac{(1-r)^2}{r^2 u_2}\right)$
Neutral	$\lvert 1-r\rvert \ll 1/N$	$N\sqrt{u_2} \ll 1$
Advantageous	$r > 1, \lvert 1-r\rvert \gg 1/N$	$Nu_1 \ll r$

- **Nearly deterministic dynamics**, Figure 4(c). For large populations ($N \gg 1/u_1$), mutants are constantly produced and steadily increase in abundance. The double-hit mutant production happens accordingly, with the mean number of two-hit mutants $\approx 1 - \exp(-Nu_1u_2rt^2/2)$.

Applications. Mathematical models described above have applications that span several different areas of oncology.

- The evolutionary dynamics of mutation generation and fixation is intimately connected with the landmark cancer phenomena of chromosomal instability and microsatellite instability. These are characterized by an increased rate of genetic changes in cells. One can argue under what circumstances the instability is an initiating and causal effect of cancer and when it is a consequence of other molecular events [**26, 33, 47**].
- Understanding the dynamics of tumor suppressor genes allows deeper understanding of the causes of many familial disorders, such as the Lynch syndrome and familial adenomatous polyposis (FAP) [**29, 34**].
- The initial steps in carcinogenesis are usually the ones that take the longest, and therefore, their signature is apparent in the population-level epidemiological data on cancer. Models of the type described here are used to relate the molecular *in vivo* processes of cancer initiation with the shape of age incidence curves [**40, 42**].
- Studying the turnover in stem cell compartments and the homeostatic control in the context of the hazard of mutant generation allows us to reason about the protective role of epithelial tissue architecture, which may in part be in place to delay the onset of deadly cancers [**59**].

Author Proof

Dynamics of stem-cell-driven cancers. The nature of the mutations that cells need to accumulate to initiate cancerous growth vary from one type of cancer to another. Some cancers have been identified as stem-cell driven, such as breast cancer [**1**], glioblastoma [**75**], and hemotopoietic cancers [**48**]; see also [**13**] for a critical review. It has been proposed that for stem-cell-driven cancers, a common crucial event is the escape from feedback loop mechanisms that prevent uncontrolled proliferation in healthy tissues and maintain tissue homeostasis. The following model [**55**] describes stem cells, S, which have unlimited reproductive potential, and differentiated cells, D, that eventually die:

$$\dot{S} = (2p(D) - 1)\, v(D)\, S, \quad \dot{D} = 2(1 - p(D))\, v(D)\, S - dD.$$

Stem cells divide at a rate v producing two stem cells with probability p or two differentiated cells with probability $(1 - p)$. Differentiated cells die at a rate d and produce factors that inhibit self-renewal and division in stem cells. The feedback loops are incorporated in the rate of cell division, $v(D)$, and the probability of self-renewal, $p(D)$, being general decreasing functions of D. To study the evolutionary dynamics of

feedback escape, we consider mutations that confer the lack of *production* of differentiation or division signals by the differentiated cells (we call these $Ddiff$ and $Ddiv$, respectively), and also mutations that confer the lack of *response* by stem cells to the differentiation or division regulating signals (mutations of type $Sdiff$ and $Sdiv$, respectively). It turns out that out of all possible mutation pathways, including these four mutation types, only one leads to uncontrolled cell growth: first the response to differentiation then to division feedback is lost. The model suggests this to be a universal pathway of feedback escape among stem-cell-driven cancers, although the nature and number of mutation events to achieve this is certainly tissue specific. Different growth patterns can result from feedback escape, which we call "inhibited," "uninhibited," and "sigmoidal." Interestingly, most growth patterns reported in the literature (both *in vivo* and *in vitro*) belong to one of the categories predicted by our model [**56**]. Examples of how observed tumor growth data (*in vivo* and *in vitro*) can be classified to one of the predicted patterns by model fitting are shown in Figure 5.

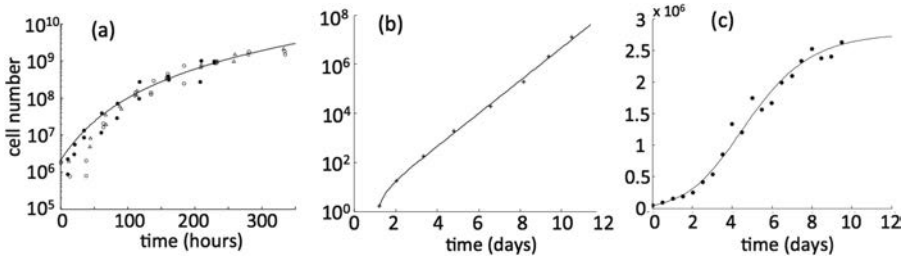

Figure 5. Experimentally observed growth patterns and model fits. (a) Inhibited growth in Ehrlich's ascites tumor [**35**]. (b) Uninhibited growth in L1210, a mouse lymphocytic leukemia [**58**]. (c) Sigmoidal growth in the nonspatial model: Jurkat T cell, human leukemia [**53**].

Author Proof

To summarize so far, we have demonstrated how computational and mathematical models can shed light onto early stages of tumor initiation and progression and inform us of the crucial events leading to cancer development.

3. ADVANCES IN MODELING TUMOR ANGIOGENESIS. An accumulation of mutations over time is required for cellular transformation and tumor initiation. These damaged cells replicate uncontrollably, eventually creating a tumor. To ensure continued growth, a tumor must acquire a sustainable supply of nutrients, and this is accomplished by recruiting new blood vessels from the nearby existing vasculature. A recent advancement in cancer treatment has been combining traditional chemotherapeutic agents with drugs that interfere with a tumor's ability to stimulate blood vessel formation. In the following section, we explore mathematical models of tumor-induced blood vessel formation and related treatment strategies.

Concepts. Angiogenesis is the formation of new blood vessels from pre-existing ones. Initiation of angiogenesis is a critical bifurcation point in tumor progression as it marks the pivotal transition from diffusion-dependent tumor growth to vascular growth, a more progressive and potentially fatal stage of the disease. The angiogenic cascade is an extremely complex, yet well-ordered, series of events involving cells that line the inner surface of blood vessel walls. To initiate angiogenesis when oxygen is scarce, tumor cells release a wide variety of angiogenic factors that stimulate blood vessel cell activation, survival, proliferation, migration, and maturation (see Figure 6). Mathematical models of angiogenesis include blood vessel cells and the chemicals that stimulate

and stabilize them as they grow toward a tumor and create an intricate new vascular network. Such models can help to answer questions like: What factors influence the distribution of cells with different behaviors in a developing sprout (quiescent cell, proliferating cell, migrating tip cell) and how can this dynamic variation be characterized? How do tip cells polarize in response to chemical gradients? How do blood vessel cells integrate the various biochemical and biomechanical cues they receive from a variety of sources in order to decide when/where to move? How do tissue properties affect angiogenesis and help to determine network structure?

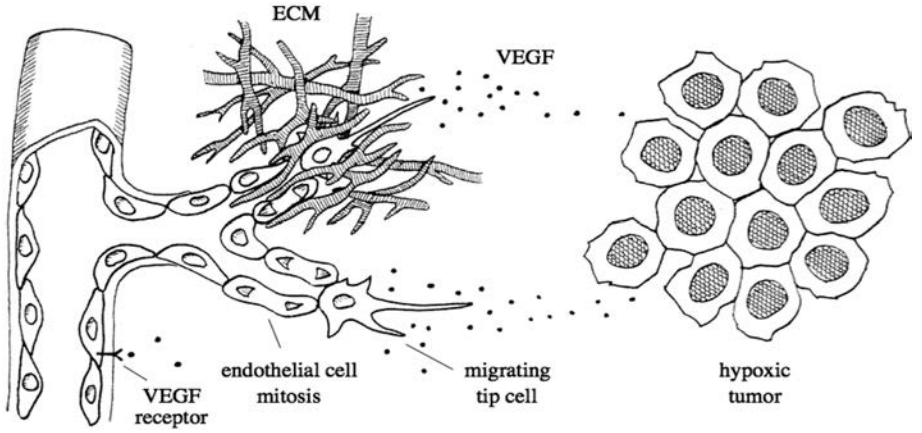

Figure 6. An illustration of early events in angiogenesis taken from [**9**]: Biochemically mediated endothelial cell activation and subsequent migration and invasion into the stroma led by tip cells extending protrusions, cell division, and endothelial cell interaction with tissue fibers. VEGF is vascular endothelial growth factor, the best characterized tumor angiogenic factor and M is the extracellular matrix or tissue fibers.

Author Proof

Mathematical modeling approaches. In the early stages of angiogenesis, recruitment of new blood vessel cells from a nearby parent vessel is the dominant mechanism for sprout extension [**4, 57**]. Subsequently, proliferation of cells in the developing sprout is essential for further spout development. Without proliferation, only a restricted sprout network is formed and eventually regresses [**60, 61, 62**]. Although the processes associated with tumor angiogenesis are the subject of many mathematical and computational investigations, few mathematical approaches, including [**2, 3, 5, 12, 11, 36, 37, 38, 49, 50, 51, 65**], are able to capture this simple, but critical, experimental observation. A detailed review of many existing tumor angiogenesis models and their limitations is provided in [**41**]. The key to resolving this problem is to derive correct relationships between cell proliferation, sprout extension, and vessel maturation, based on experiments. In order to untangle some of the complexities of tumor angiogenesis and in hopes of manipulating new knowledge for therapeutic gain, new mathematical modeling frameworks that operate at the molecular and cellular level must be developed [**9, 10, 23, 24, 25**]. This is critical because it is precisely this level of detail that is necessary to accurately predict the therapeutic potential of novel molecular targets aimed at angiogenesis.

One way to do this is to adopt a cell-based approach that integrates the mechanical aspects of cell elongation with a biochemical model of dynamic variation in cellular behaviors. This type of approach is used in [**23**], and there are many important features of this angiogenesis model that are entirely new, including the derivation, from general viscoelastic equations, of a force balance equation for tip cell elongation and the

model mechanism for nonproliferative sprout extension. The computational domain is a square, in which a tumor is represented by a disc with radius r. Angiogenic factors are produced by cells, and then they can diffuse, decay, and be taken up by cells. These are continuous processes, and therefore they are modeled by partial differential equations (PDEs). Newly forming vascular sprouts are divided into two parts: a tip cell and stalk cells. Each stalk cell grows, and once its mass is doubled, it divides into two equal-mass daughter cells, which will redistribute in space. This phenomenon is almost impossible to capture using a continuous model. Therefore, discrete points are used to track all of the cells in the vessel, and on each discrete point (one cell) of the vessel stalk, a time-continuous mass density and local mature cell mass fraction are assigned and modeled using PDEs.

In this way, the model is a hybrid formulation containing both continuous (diffusion of chemicals) and discrete (cells) components. A cell-based approach is also employed as the tip cell is modeled as a spring-dashpot system [**39, 40**], which is a common approach in mechanics used to describe the elastic and viscous components of the stress/stain response. Using this formulation, cells generate a protrusion force, F, so that the elongation of the cell body, u, satisfies the force balance equation:

$$\frac{EA_0}{L_0}u + \frac{\mu A_0}{L_0}\frac{du}{dt} + \beta A_1 \frac{du}{dt} = \mathbf{K} \circ F. \tag{1}$$

The first term is the elastic force of the spring followed by the internal viscous force (the second term). The third term is the friction or drag on the contact surface with of tissue fibers, and the last term, $\mathbf{K} \circ F$, is the chemotactic force. This equation can be rigorously derived from the viscoelastic model with small deformation with variables defined as follows: Youngs modulus E, viscosity μ, friction between ECs and tissue fibers β, cross-sectional area A_0 of the tip cell, initial length of the cell L_0, and contact area of cellular extensions with ECM A_1. In multidimensional space, $\mathbf{K}$ is called a conductivity tensor, and it accounts for contact guidance along tissue fibers.

The integrated model combines the migration, proliferation, and maturation processes described above. Immediately after a cell divides, the new cells are round in shape and easily deformed; therefore, under the chemotactic force, they will be stretched toward the tip, which allows the tip cell to retract and migrate again. By repeating this process, the sprout extends to the source of chemoattractant, and this extension is tracked in time and space. This model is able to provide insights into the relative impact of endothelial cell proliferation, migration, and maturation during tumor angiogenesis. Validation was achieved by quantitatively comparing model predictions to data derived from corneal angiogenesis experiments (Figure 7) and was used to investigate the effects of the X-ray irradiation, chemical inhibition, and extracellular matrix anisotropy on sprout morphology and extension.

Applications. This modeling approach that captures the multiscale processes associated with angiogenesis at the molecular and cellular level can now be combined and integrated with mathematical models for solid tumor growth like those developed in [**19, 64**]. Such an integrative computational modeling framework will be able to mechanistically follow tumor progression from the avascular stage of growth through the angiogenic switch to rapid vascular growth to therapeutic tumor reduction. There are data available to calibrate and validate the computational predictions, and model output can be directly compared to published experimental observations of tumor size, weight vascular density following treatment with a variety of currently approved single and multidrug strategies [**15, 18, 39, 46, 73**].

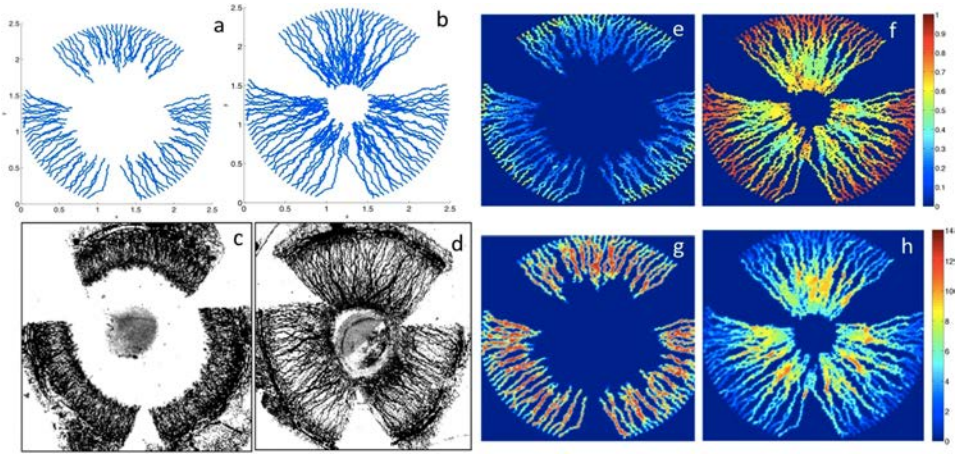

Figure 7. Simulation of normal growth taken from [**23**]. (a) On day 4, there are 90 vessels with average length 0.53 (=1.06*mm*). (b) On day 7, there are 227 vessels with average length 0.92 (=1.84*mm*). (c)&(d): Experimental results on day 4 and 7 from [**72**]. Right panel (e)&(f): Quiescent level, which is a measure of cell maturity. (g)&(h): chemical concentration along the sprout.

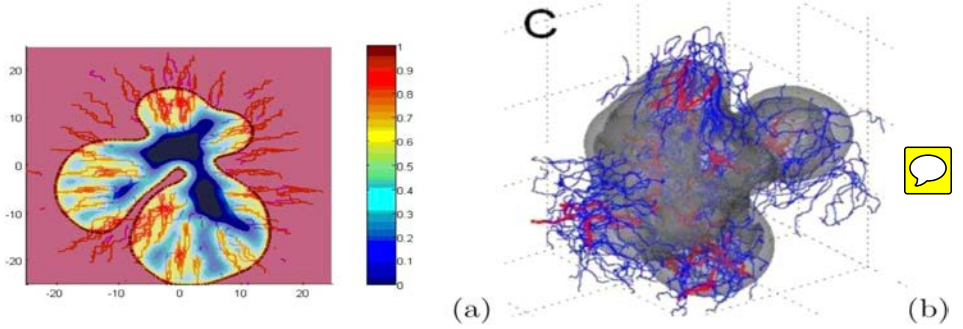

Figure 8. Simulations of vascular tumor growth from (a) [**64**] and (b) [**19**].

Once validated, this modeling approach will also be poised to investigate the effect of novel molecular targets aimed at tumor angiogenesis. This is precisely the level of detail that is necessary to accurately incorporate drug mechanism of action and predict the therapeutic potential. For example, these models can be used to predict response to therapeutic blockage of proteins associated with vessel maturation and cell survival and can pinpoint the quantifiable differences in vascular composition of single-target approaches versus multitarget therapies. AQ2

4. PATIENT-SPECIFIC MATHEMATICAL ONCOLOGY. Traversing the chasm between biological discoveries and their clinical translation is a major challenge facing oncology. We believe that clinical translation of biomedical discoveries can be enabled by using mathematical modeling as a bridge between cancer biology and clinical oncology. Primary brain tumors known as gliomas are a particularly challenging case as little improvement in outcomes has been seen in decades of study. While clinical trials of treatment for gliomas have continued to focus on statistically defined results in groups of similar patients, we have focused on trying to understand individual cases by pioneering the field of patient-specific mathematical neuro-oncology [**6, 7, 8, 14, 21, 22, 44, 45, 54, 68, 69, 70, 71, 74**]. Since routine clinical data on

patients are limited, one has to carefully balance the biological detail captured by the model, in the form of model complexity, with our ability to parameterize the model for each patient. As such, we have developed and applied mathematical models of glioma proliferation and invasion to generate simulations of untreated tumor growth for each patient.

To reasonably calibrate these models to each patient's tumor, we have focused on models that can be informed by information routinely available to patients—clinical imaging, usually in the form of magnetic resonance imaging (MRI). Since MRIs can only resolve to roughly a cubic millimeter scale, which likely contains many thousands of cells, it is important for our mathematical model to be on a similar scale-continuum of cells. For this reason, much of our investigations has focused on minimal reaction-diffusion continuum models of the form

$$\overbrace{\frac{\partial c}{\partial t}}^{\text{change of tumor cell density}} = \overbrace{\nabla \cdot (\mathbf{D}\nabla c)}^{\text{net dispersal of tumor cells}} + \overbrace{\rho c\left(1-\frac{c}{K}\right)}^{\text{net proliferation of tumor cells}}$$

where $\mathbf{D}$ is the net dispersal rate of the tumor cells c, ρ is the net proliferation rate of the tumor cells, and K is the maximal carrying capacity of tumor cells the tissue can accommodate. Although extensions to this base model formalism are actively used, this simple model serves as an ideal base for investigating patient-specific tumor kinetics observed on MRI. Specifically, to produce patient-specific virtual controls, we calibrate our tissue-scale models of tumor growth to routinely obtained clinical imaging, primarily MRIs obtained prior to treatment. Specifically, calibration involves estimating the model parameters (D, ρ, etc.) for each patient. Here we highlight a series of successes these modeling efforts have brought to the face of clinical decision making for gliomas.

Author Proof

Predicting the invisible: Identifying the patients most likely to benefit from extensive surgery. The standard-of-care for high-grade gliomas (HGGs) includes resection of the enhancing component of the tumor visible on gadolinium-enhanced T1-weighted MRI [**67**] yet imaging reveals only the tip of the iceberg of this disease. That is, there is an unknown extent of diffusely invaded glioma cells even several centimeters peripheral to the abnormality seen on imaging. Worse yet, the degree of invasion is highly variable across patients. As a result of the variability of diffuse tumor cell invasion (D) across patients, surgical interventions are led by a combination of the clinically imageable extent of disease (bright region on the contrast-enhanced T1-weighted MRI) and the eloquence (and therefore resectability) of the brain tissue surrounding that imaging nodule.

Using our mathematical models for glioma proliferation and invasion, we have generated patient-specific simulations of the degree of diffuse invasion peripheral to the imaging abnormality for HGGs. The top row of Figure 9 shows several slices of an MRI of a patient with a fronto-temporal HGG whereas the bottom row shows the diffuse extent predicted by the model (approximated by D/ρ) calibrated to this patient using calibration methods developed in [**6, 7, 8, 14, 21, 22, 44, 45, 54, 68, 69, 70, 71, 74**]. In a study of 250 HGGs [**6**], by ordering these tumors according to their patient-specific degree of invasiveness, termed the invisibility index (D/ρ) [**6, 7, 20, 71**], we were able to identify a subset of patients predicted to have a minimal extent of diffuse invasion. Patients with these so-called nodular tumors, when treated with gross total resection of the imageable nodule, experienced an average 8 months, or 75%, increase in survival whereas the most diffuse tumors, received no measurable survival benefit.

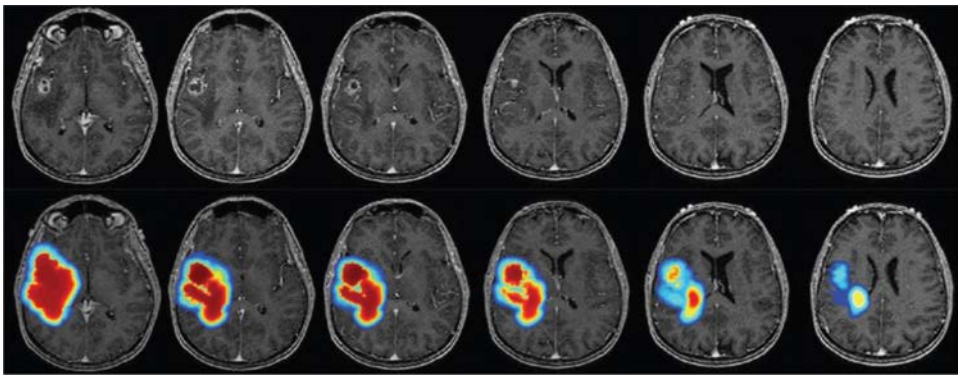

Figure 9. Top: Gadolinium-enhanced T1-weighted MRI showing a right fronto-temporal contrast-enhancing lesion. Bottom: Patient-specific simulation showing diffuse invasion color coded for cell density with red corresponding to high and blue low.

Combining our ability to estimate patient-specific invisibility index (D/ρ) with these patient observations suggests an obvious clinical trial in which patients are stratified according to their model-predicted diffuse extent to prospectively identify which patients will most benefit from significant surgical resection.

Optimizing radiation therapy to maximally benefit each patient. After resection, essentially all high-grade glioma patients receive radiotherapy, yet, similar to resection, there is very little patient-specific tuning to optimize the therapy to maximally benefit the patient. We have used patient-specific modeling as a means to provide alternates to these one-size-fits-all radiation treatment design strategies. Specifically, by incorporating a model for radiotherapy response (cell kill) into our patient-specific model, we can capture the kinetics of radiotherapy response in individual patients [**54**].

Author Proof

$$\overbrace{\frac{\partial c}{\partial t}}^{\text{change of tumor cell density}} = \overbrace{\nabla \cdot (\mathbf{D}(x)\nabla c)}^{\text{net dispersal}} + \overbrace{\rho c\left(1-\frac{c}{K}\right)}^{\text{net proliferation}} - \overbrace{R(c,x,t)}^{\text{response to radiation}}$$

Using this model and pretreatment MRIs, we are able to predict early postradiotherapy imaging within a few millimeters of accuracy [**54**]. We further used this predictive relationship in combination with multi-objective optimization to generate optimal radiation schedules to increased predicted tumor response of 21% to 105% while decreasing radiation exposure to normal tissue by 67% to 93% [**14, 22**]. These results are ripe for clinical trials to assess the benefit of these altered therapy plans in cohort of glioma patients.

Quantifying treatment response using untreated virtual controls. Another major clinical challenge facing gliomas is the lack of useful response metrics that connect treatment response to survival and other outcomes. That is, there are few early signs of treatment response that portend for ultimate benefit in terms of overall survival [**52, 76**]. We recently developed a method to use patient-specific simulations of untreated tumor growth, tuned to each patients estimated D and ρ as a so-called virtual control against which treatment response can be assessed. Simply by comparing post-treatment imaging to the simulated prediction of the untreated virtual control, one can assess the degree of tumor growth deflection as a result of treatment to generate novel response metrics (Figure 10). Importantly, these virtual control-based response metrics

are strong predictors of overall survival [**44, 45**]. We believe that these response metrics could be used across much of neuro-oncology to enable the early identification of therapies that benefit individual patients with the major exception of antiangiogenics.

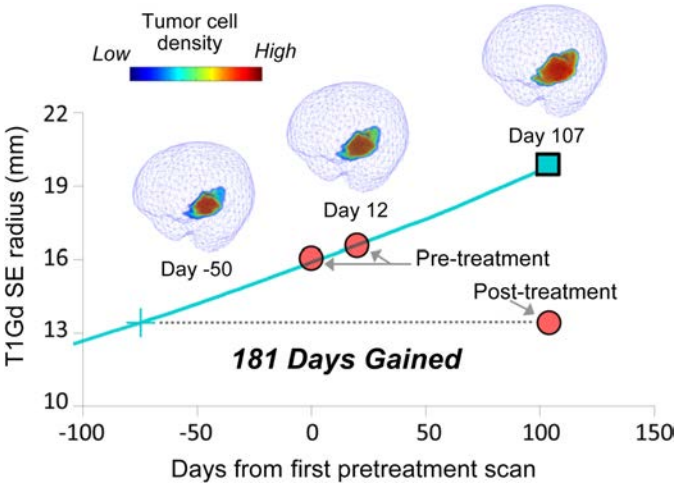

Figure 10. Patient-specific 4D simulation of tumor growth and progression shown in 3D brain outlines with the mean model-predicted radius of the imageable lesion shown as a cyan curve evolving with time. The sizes of the tumor on pre-treatment and post-treatment MRIs are shown as red circles showing that there was a 181 days of deflection of tumor growth from the untreated path (cyan) as a result of the intervening therapy. Image adapted from [**44**].

Author Proof

Deconvolving tumor growth from imaging changes during treatment with antiangiogenics. As is clear from the above, much of neuro-oncology relies on clinical imaging, particularly contrast-enhancement and surrounding edema on different MRI modalities. Interestingly, contrast-enhancement is a result of leakage of a contrast agent from angiogenic neovasculature in the tumor,which also allows leakage of edematous liquid into the surrounding brain. Thus, not only does angiogenesis play a critical role in tumor growth, it also plays a crucial role in our ability to image the disease. This deep connection between tumor biology and imaging is further confounded when we treat with antiangiogenics such as Avastin (bevacizumab) where the imaging signal can decrease as if the tumor was regressing when it may not be. To this end, enabled by the excellent modeling work done on VEGF-mediated angiogenesis by Jackson et al (above), we extended our glioma model to incorporate the generation of edema to more directly reflect the imaging changes seen before and during antiangiogenic therapy [**21**]. Figure 11 illustrates how simulations of this model allow one to decouple changes in edema patterns on MRI from the actual tumor progression. This allows for a direct appreciation of the complex relationship between imaging and actual tumor extent that is directly targeted at the clinical challenge of interpreting imaging changes with antiangiogenic therapy and identifying patients who will maximally benefit.

5. THE FUTURE OF CANCER MODELING. We have described mathematical and computational approaches that integrate biological data and imaging to answer questions about tumor initiation, vascularization, and patient specific therapy. The future of mathematical oncology promises innovations and new challenges in all of these areas.

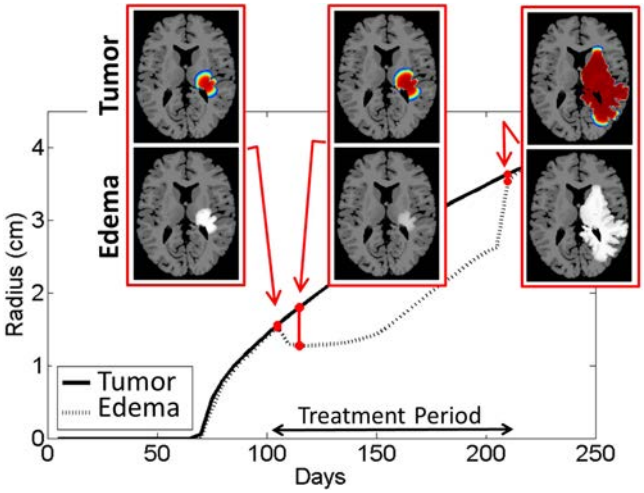

Figure 11. Top: Simulated tumor growth (red as high cell density while blue is low) Bottom: Imageable response to antiangiogenic therapy showing a significant imaging response while the tumor growth is undetectably deflected. Image adapted from [**21**].

Stochastic evolutionary models of carcinogenesis are unique in a sense that they combine a large degree of reductionism (the simplicity of the model setting) with a high degree of analytical tractability, simultaneously providing insights into unknown aspects of carcinogenesis. Starting from seminal works of Knudson and Moolgavkar, models of this type have provided a window into the microscopic tumor dynamics, when applied to population level data. Similarly to using epidemiological data, one can infer underlying microscopic processes by directly comparing predicted model behavior with observed tumor growth kinetics *in vivo*.

For example, by matching the observed growth data of stem-cell-driven tumors with predicted patterns, we can gain insights about the nature of the evolutionary changes that have occurred in the tumor under consideration. This, in turn, is part of a larger concept, where analysis of cellular growth data can be used to infer the types of evolutionary changes that have occurred in cancers, an idea recently proposed in [**56**]. Simplicity and complexity must strike the right balance in future modeling work. Using the basic evolutionary models such as the ones described here, one can try to build in more and more biologically relevant details, without losing track of causality and tractability of the system.

As with models of carcinogenesis, we are also on the verge of many exciting advances in modeling tumor angiogenesis and subsequent vascular tumor growth. Computational modeling frameworks can mechanistically follow tumor progression from the avascular stage of growth, through the angiogenic switch, to rapid vascular growth. We expect the future to bring new approaches that accurately simulate angiogenesis-dependent vascular tumor growth in greater detail than any current model in the literature. These models will be able to capture molecular, cellular and tissue level details, which are crucial to addressing the therapeutic potential of molecular targets that are yet to be discovered.

Ultimately, outcomes for all cancers are a product of tumor biology (growth) and response to therapy. Since there is no practical means to define these variables in isolation for an individual patient, the creation of a virtual tumor through application of a well-described mathematical model provides an immediate means to investigate the interplay of biology and response in outcomes. We believe that such models

can form the basis of a spectrum of clinical trials to improve outcomes for patients battling cancer. As such, the field of mathematical oncology has the opportunity to drive forward a completely new trajectory of precision treatment strategies for cancer patients.

REFERENCES

1. M. Al-Hajj, M. S. Wicha, A. Benito-Hernandez, S. J. Morrison, M. F. Clarke, Prospective identification of tumorigenic breast cancer cells, *Proc. Nat. Acad. Sci. USA* **100** (2003) 3983–3988, http://dx.doi.org/10.1073/pnas.0530291100.
2. A. R. A. Anderson, M. A. J. Chaplain, Continuous and discrete mathematical models of tumor-induced angiogenesis, *Bull. Math. Biol.* **60** (1998) 857–900, http://dx.doi.org/10.1006/bulm.1998.0042.
3. ———, A mathematical model for capillary network formation in the absence of endothelial cell proliferation, *Appl. Math. Lett.* **11** (1998) 109–114, http://dx.doi.org/10.1016/s0893-9659(98)00041-x.
4. D. H. Ausprunk, J. Folkman, Migration and proliferation of endothelial cells in preformed and newly-formed blood vessels during tumor angiogenesis, *Microvasc. Res.* **14** (1977) 53–65.
5. D. Balding, D. L. S. McElwain, A mathematical model of tumor-induced capillary growth, *J. Theor. Biol.* **114** (1985) 53–73, http://dx.doi.org/10.1016/s0022-5193(85)80255-1.
6. A. L. Baldock, S. Ahn, R. Rockne, M. Neal, D. Corwin, K. Clark-Swanson, G. Sterin, A. D Trister, H. Malone, V. Ebiana, A. M. Sonabend, M. Mrugala, J. K. Rockhill, D. L. Silbergeld, A. Lai, T. Cloughesy, G. M. McKhann, J. N, Bruce, R. Rostomily, P. Canoll, K. R. Swanson, Patient-specific metrics of invasiveness reveal significant prognostic benefit of resection in a predictable subset of gliomas, *PLoS One* (forthcoming).
7. A. L. Baldock, R. C. Rockne, A. D. Boone, M. L. Neal, A. Hawkins-Daarud, D. M. Corwin, C. A. Bridge, L. A. Guyman, A. D. Trister, M. M. Mrugala, J. K. Rockhill, K. R. Swanson, From patient-specific mathematical neuro-oncology to precision medicine, *Front Oncol* **3** (2013), http://dx.doi.org/10.3389/fonc.2013.00062.
8. A. L. Baldock, K. Yagle, D. E. Born, S. Ahn, A. D. Trister, M. Neal, S. K. Johnston, C. A. Bridge, D. Basanta, J. Scott, H. Malone, A. M. Sonabend, P. Canoll, M. M. Mrugala, J. K. Rockhill, R. C. Rockne, K. R. Swanson, Invasion and proliferation kinetics in enhancing gliomas predict IDH1 mutation status, *Neuro-Oncology* **16** (2014) 779–786, http://dx.doi.org/10.1093/neuonc/nou027.
9. A. Bauer, T. Jackson, Y. Jiang, A cell-based model exhibiting branching and anastomosis during tumor-induced angiogenesis, *Biophysical Journal* **92** (2007) 3105–3121, http://dx.doi.org/10.1529/biophysj.106.101501.
10. ———, Topography of extracellular matrix mediates vascular morphogenesis and migration speeds, *PLoS* **5** no. 7 (2009), http://dx.doi.org/10.1371/journal.pcbi.1000445.
11. H. M. Byrne, M. A. J. Chaplain, Explicit solutions of a simplified model of capillary sprout growth during tumor angiogenesis, *Appl. Math. Lett.* **9** (1996) 69–74, http://dx.doi.org/10.1016/0893-9659(95)00105-0.
12. ———, Mathematical models for tumour angiogenesis: Numerical simulations and nonlinear wave solutions, *Bull. Math. Biol.* **57** (1995) 461–486, http://dx.doi.org/10.1016/s0092-8240(05)81778-1.
13. H. Clevers, The cancer stem cell: premises, promises and challenges, *Nature Medicine* (2011) 313–319, http://dx.doi.org/10.1038/nm.2304.
14. D. Corwin, C. H. Holdsworth, R. Stewart, M. Philips, R. Rockne, K. Swanson, Using a patient-specific mathematical model and a multiobjective IMRT optimization algorithm in treatment planning for human glioblastoma, *Int. J. Rad. Oncol. Biol. Phys.* **87** (2013) S257–S257, http://dx.doi.org/10.1016/j.ijrobp.2013.06.669.
15. M. H. Dastierdi, K. M. Al-Arfai, N. Nallasamy, Topical bevacizumab in the treatment of corneal neovascularization, *Arch Ophthalmolr* **127** (2009) 381–389, http://dx.doi.org/10.1001/archophthalmol.2009.18.
16. R. Durrett, J. Foo, K. Leder, Spatial Moran models II. tumor growth and progression, submitted.
17. D. Wodarz, N. L. Komarova, Spatial moran models I. stochastic tunneling in the neutral case, *Ann. Appl. Probab.* (forthcoming).
18. B. L. Falcón, H. Hashizume, P. Koumoutsakos, J. Chou, Contrasting actions of selective inhibitors of angiopoietin-1 and angiopoietin-2 on the normalization of tumor blood vessels, *Am. J. Pathol.* **175** (2009) 2159–2170,http://dx.doi.org/10.2353/ajpath.2009.090391.

Author Proof

19. H. Frieboes, J. S. Lowengrub, S. Wise, X. Zheng, Computer simulation of glioma growth and morphology, *Neuroimage* **37** (2007) S59–S70, http://dx.doi.org/10.1016/j.neuroimage.2007.03.008.
20. H. L. Harpold, E. C. Alvord, Jr., K. R. Swanson, The evolution of mathematical modeling of glioma proliferation and invasion, *J. Neuropathol Exp. Neurol* **66** (2007) 1–9, http://dx.doi.org/10.1097/nen.0b013e31802d9000.
21. A. Hawkins-Daarud, R. C. Rockne, A. R. Anderson, K. R. Swanson, Modeling tumor-associated edema in gliomas during anti-angiogenic therapy and its impact on imageable tumor, *Front Oncol* **3** (2013), http://dx.doi.org/10.3389/fonc.2013.00066.
22. C. H. Holdsworth, D. Corwin, R. D. Stewart, R. Rockne, A. D. Trister, K. R. Swanson, M. Phillips, Adaptive IMRT using a multiobjective evolutionary algorithm integrated with a diffusion-invasion model of glioblastoma, *Phys Med Biol* **57** (2012) 8271–8283, http://dx.doi.org/10.1088/0031-9155/57/24/8271.
23. T. L. Jackson, X. Zheng, A cell-based model of endothelial cell elongation, proliferation and maturation during corneal angiogenesis, *Bull. Math. Biol.* **72** (2010) 830–868, http://dx.doi.org/10.1007/s11538-009-9471-1.
24. ———, A hybrid mathematical model of endothelial cell elongation, proliferation and maturation during corneal angiogenesis, *DCDS-B* **18** (2013) 1109–1154.
25. H. V. Jain, J. E. Nör, T. L. Jackson, Modeling the VEGF–Bcl-2–CXCL8 pathway in intratumoral angiogenesis, *Bull. Math. Biol.* **70** (2008) 89–117, http://dx.doi.org/10.1007/s11538-007-9242-9.
26. N.L. Komarova, A. V. Sadovsky, F. Y. Wan, Selective pressures for and against genetic instability in cancer: A time-dependent problem, *J of The Royal Society Interface* **5** (2008) 105–121, http://dx.doi.org/10.1098/rsif.2007.1054.
27. N. L. Komarova, Spatial stochastic models for cancer initiation and progression, *Bull. Math. Bio.* **68** (2006) 1573–1599, http://dx.doi.org/10.1007/s11538-005-9046-8.
28. ———-, Stochastic modeling of loss-and gain-of-function mutations in cancer, *Math. Models Methods Appl. Sci.* **17** (2007) 1647–1673, http://dx.doi.org/10.1142/s021820250700242x.
29. N. L. Komarova, C. Lengauer, B. Vogelstein, M. A. Nowak, Dynamics of genetic instability in sporadic and familial colorectal cancer, *Cancer Biology & Therapy* **1** (2002) 685–692, http://dx.doi.org/10.4161/cbt.321.
30. N. L. Komarova, A. Sengupta, M. A. Nowak, Mutation–selection networks of cancer initiation: Tumor suppressor genes and chromosomal instability, *J. Theoretical Biol.* **223** (2003) 433–450, http://dx.doi.org/10.1016/s0022-5193(03)00120-6.
31. N. L. Komarova, L. Shahriyari, D. Wodarz, Complex role of space in the crossing of fitness valleys by asexual populations, *J. Roy. Soc. Interface* **95** (2014) 20140014, http://dx.doi.org/10.1098/rsif.2014.0014.
32. N. L. Komarova, L. Wang, Initiation of colorectal cancer: Where do the two hits hit?, *Cell Cycle* **3** (2004) 1558–1565, http://dx.doi.org/10.4161/cc.3.12.1186.
33. N. L. Komarova, D. Wodarz, The optimal rate of chromosome loss for the inactivation of tumor suppressor genes in cancer, *Proc. Nat. Acad. Sci. USA* **101** (2004) 7017–7021, http://dx.doi.org/10.1073/pnas.0401943101.
34. N. L. Komarova, D. Wodarz, C. R. Boland, A. Goel, Genetic and epigenetic pathways to colon cancer relating experimental evidence with modeling, in *Selected Topics in Cancer Modeling*. Springer, Birkhäuser, Boston, 2008.
35. K. A. Laird, Dynamics of tumour growth, *Brit. J. Cancer* **18** (1964) 490.
36. H. A. Levine, M. Nilsen-Hamilton, Angiogenesis—A biochemial/mathematical perspective, in *Tutorials in Mathematical Biosciences III*. Edited by A. Friedman. no. 1872. Lecture Notes in Mathematics. Springer, 2006.
37. H. A. Levine, S. Pamuk, B. D. Sleeman, M. Nilsen-Hamilton, Mathematical modeling of capillary formation and development in tumor angiogenesis: penetration into the stroma, *Bull. Math. Biol* **63** (2001) 801–863, http://dx.doi.org/10.1006/bulm.2001.0240.
38. H. A. Levine, B. D. Sleeman, M. Nilsen-Hamilton, Mathematical modeling of the onset of capillary formation initiating angiogenesis, *J. Math. Biol.* **42** (2001) 195–238, http://dx.doi.org/10.1007/s002850000037.
39. M. H. G. Longenberg, P. O. Witteveen, N. A. G. Lankheet, Phase 1 study of combination treatment with PTK 787/ZK 222584 and cetuximab for patients with advanced solid tumors: safety, pharmacokinetics, pharmacodynamics analysis, *Neoplasia* **12** (2010) 206–213.
40. G. E. Luebeck, S. J. Moolgavkar, Multistage carcinogenesis and the incidence of colorectal cancer, *Proc. Nat. Acad. Sci. USA* **99** (2002) 15095–15100, http://dx.doi.org/10.1073/pnas.222118199.
41. N. Mantzaris, S. Webb, H. G. Othmer, Mathematical modeling of tumor-induced angiogenesis, *J. Math Biol.* **49** (2004) 111–187, http://dx.doi.org/10.1007/s00285-003-0262-2.

Author Proof

42. R. Meza, J. Jeon, S. H. Moolgavkar, G. E. Luebeck, Age-specific incidence of cancer: Phases, transitions, and biological implications, *PNAS* **105** (2008) 16284–16289, http://dx.doi.org/10.1073/pnas.0801151105.
43. P. A. P. Moran, *The Statistical Processes of Evolutionary Theory*. Clarendon Press, Oxford, 1962.
44. M. L. Neal, A. D. Trister, S. Ahn, A. Baldock, C. A. Bridge, L. Guyman, J. Lange, R. Sodt, T. Cloke, A. Lai, T. F. Cloughesy, M. M. Mrugala, J. K. Rockhill, R. C. Rockne, K. R. Swanson, Response classification based on a minimal model of glioblastoma growth is prognostic for clinical outcomes and distinguishes progression from pseudoprogression, *Cancer Res* **73** (2013) 2976–2986, http://www.ncbi.nlm.nih.gov/pubmed/23400596.
45. M. L. Neal, A. D. Trister, S. Ahn, A. Baldock, C. A. Bridge, R. Sodt, T. Cloke, A. Lai, T. F. Cloughesy, M. M. Mrugala, J. K. Rockhill, R. C. Rockne, K. R. Swanson, Discriminating survival outcomes in patients with glioblastoma using a simulation-based, patient-specific response metric, *PLoS One* **8** (2013) e51951, http://dx.doi.org/10.1371/journal.pone.0051951.
46. J. E. Nör, J. Christensen, J. Liu, Up-regulation of bcl-2 in microvascular endothelial cells enhances intratumoral angiogenesis and accelerates tumor growth, *Cancer Res.* **61** (2001) 2183–2188.
47. M. A. Nowak, N. L. Komarova, A. Sengupta, P. V. Jallepalli, The role of chromosomal instability in tumor initiation, *Proc. Nat. Acad. Sci. USA* **99** (2002) 16226–16231, http://dx.doi.org/10.1073/pnas.202617399.
48. E. Passegué, C. H. M. Jamieson, L. E. Ailles, I. L. Weissman, Normal and leukemic hematopoiesis: Are leukemias a stem cell disorder or a reacquisition of stem cell characteristics?, *Proc. Nat. Acad. Sci. USA* **100** (2003) 11842–11849.
49. M.J. Plank, B.D. Sleeman, Lattice and non-lattice models of tumour angiogenesis, *Bull. Math. Biol.* **66** (2004) 1785–1819, http://dx.doi.org/10.1016/j.bulm.2004.04.001.
50. ———, A reinforced random walk model of tumor angiogenesis and anti-angiogenesis strategies, *IMA J. Math. Med. Biol.* **20** (2003) 135–181, http://dx.doi.org/10.1093/imammb20.2.135.
51. M.J. Plank, B.D. Sleeman, P. F. Jones, A mathematical model of tumour angiogenesis, regulated by vascular endothelial growth factor and the angiopoietins, *J. Theor. Biol.* **229** (2004) 435–454, http://dx.doi.org/10.1016/j.jtbi.2004.04.012.
52. E. C. Quant, P. Y. Wen, Response assessment in neuro-oncology, *Curr Oncol Rep* **13** (2010) 50–56, http://dx.doi.org/10.1007/s11912-010-0143-y.
53. R. Reuss, J. Ludwig, R. Shirakashi, F. Ehrhart, Intracellular delivery of carbohydrates into mammalian cells through swelling-activated pathways, *J. Membrane Biol.* **200** (2004) 67–81, http://dx.doi.org/10.1007/s00232-004-0694-7.
54. R. Rockne, J. K. Rockhill, M. Mrugala, A. M. Spence, I. Kalet, K. Hendrickson, A. Lai, T. Cloughesy, E. C. Alvord, K. R. Swanson, Predicting the efficacy of radiotherapy in individual glioblastoma patients in vivo: A mathematical modeling approach, *Phys. Med. Biol.* **55** (2010) 3271–3285, http://dx.doi.org/10.1088/0031-9155/55/12/001.
55. I. A. Rodriguez-Brenes, N. L. Komarova, D. Wodarz, Evolutionary dynamics of feedback escape and the development of stem-cell-driven cancers, *Proc. Nat. Acad. Sci. USA* **108** (2011) 18983–18988, http://dx.doi.org/10.1073/pnas.1107621108.
56. ———, Tumor growth dynamics: Insights into evolutionary processes, *Trends Ecol. Evolution* **28** (2013) 597–604, http://dx.doi.org/10.1016/j.tree.2013.05.020.
57. C. E. Semino, R. D. Kamm, D. A. Lauffenburger, Autocrine EGF receptor activation mediates endothelial cell migration and vascular morphogenesis induced by VEGF under interstitial flow, *Exp. Cell Res.* **312** (2006) 289–298, http://dx.doi.org/10.1016/j.yexcr.2005.10.029.
58. S. E. Shackney, A computer model for tumor growth and chemotherapy, and its application to L1210 leukemia treated with cytosine arabinoside (NSC-63878), *Cancer Chemotherapy Reports* **54** (1970) 399.
59. L. Shahriyarii, N. L. Komarova, Symmetric vs asymmetric stem cell divisions: an adaptation against cancer?, *PLoS One* **8** (2013) e76195, http://dx.doi.org/10.1371/journal.pone.0076195.
60. M. M. Sholley, G. P. Ferguson, H. R. Seibel, J. L. Montour, J. D. Wilson, Mechanisms of neovascularization. Vascular sprouting can occur without proliferation of endothelial cells, *Lab. Invest.* **51** (1984) 624–634.
61. M. M. Sholley, J. D. Wilson, J. L. Montour, Effect of X-Irradiation on proliferation of microvascular endothelial cells, *Rad. Res.* **94** (1983) 648–649.
62. ———, Microvascular growth in X-irradiated rat corneas, *Rad. Res.* **94** 649.
63. R. Siegel, J. Ma, Z. Zou, A. Jemal, Cancer Statistics, 2014, *CA Cancer J Clin* **64** (2014) 9–29.
64. J. P. Sinek, S. Sanga, X. Zheng, H. B. Frieboes, M. Ferrari, V. Cristini, Predicting drug pharmacokinetics and effect in vascularized tumors using computer simulation, *J. Math Biol.* **58** (2009) 485–510, http://dx.doi.org/10.1016/j.nano.2006.10.048.

Author Proof

65. B. D. Sleeman, I. P. Wallis, Tumour induced angiogenesis as a reinforced random walk: Modeling capillary network formation without endothelial cell proliferation, *J. Math. Comp. Modelling* **36** (2002) 339–358, http://dx.doi.org/10.1016/s0895-7177(02)00129-2.
66. T. Strachan, A. P. Read, *Human Molecular Genetics*, BIOS Scientific, New York, 1996.
67. R. Stupp, W. P. Mason, M. J. van den Bent, M. Weller, B. Fisher, M. J. Taphoorn, K. Belanger, Radiotherapy plus concomitant and adjuvant temozolomide for glioblastoma, *N Engl J Med* **352** (2005) 987–996.
68. K. R. Swanson, *Mathematical Modeling of the Growth and Control of Tumors*, Ph.D. thesis, University of Washington, Seattle, WA, 1999.
69. K. R. Swanson, H. L. Harpold, D. L. Peacock, R. Rockne, C. Pennington, L. Kilbride, R. Grant, J. M. Wardlaw, E. C. Alvord, Jr., Velocity of radial expansion of contrast-enhancing gliomas and the effectiveness of radiotherapy in individual patients: A proof of principle, *Clin Oncol* **20** no. 4 (2008) 301–308.
70. K. R. Swanson, K. C. Rockne, J. Claridge, M. A. Chaplain, E. C. Alvord, A. R. Anderson, Quantifying the role of angiogenesis in malignant progression of gliomas: In silico modeling integrates imaging and histology, *Cancer Res* **71** no. 24 (2011) 7366–7375, http://dx.doi.org/10.1158/0008-5472.can-11-1399.
71. M. D. Szeto, G. Chakraborty, J. Hadley, R. Rockne, M. Muzi, E. C. Alvord, Jr. K. A. Krohn, A. M. Spence, K. R. Swanson, Quantitative metrics of net proliferation and invasion link biological aggressiveness assessed by MRI with hypoxia assessed by FMISO-PET in newly diagnosed glioblastomas, *Cancer Res* **69** no. 10 (2009) 4502–4509, http://dx.doi.org/10.1158/0008-5472.can-08-3884.
72. L. J. Thompson, F. Wang, A. D. Proia, Proteome analysis of the rat cornea during angiogenesis, *Proteomics* **3** (2003) 2258–2266, http://dx.doi.org/10.1002/pmic.200300498.
73. L. von Baumgarten, D. Brucker, A. Tirniceru, Bevacizumab has differential and dose-dependent effects on glioma blood vessels and tumor cells, *Clin. Cancer Res.* **17** (2011) 6192–6205, http://dx.doi.org/10.1158/1078-0432.ccr-10-1868.
74. C. H. Wang, J. K. Rockhill, M. Mrugala, D. L. Peacock, A. Lai, K. Jusenius, J. M. Wardlaw, T. Cloughesy, A. M. Spence, R. Rockne, E. C. Alvord, Jr., K. R. Swanson, Prognostic significance of growth kinetics in newly diagnosed glioblastomas revealed by combining serial imaging with a novel biomathematical model, *Cancer Res* **69** no. 23 (2009) 9133–9140, http://dx.doi.org/10.1158/0008-5472.can-08-3863.
75. R. Wang, K. Chadalavada, J. Wilshire, U. Kowalik, K. E. Hovinga, A. Geber, B. Fligelman, M. Leversha, C. Brennan, V. Tabar, Glioblastoma stem-like cells give rise to tumour endothelium, *Nature* **468** no. 7325 (2010) 829–833, http://dx.doi.org/10.1038/nature09624.
76. P. Y. Wen, A. D. Norden, J. Drappatz, E. Quant, Response assessment challenges in clinical trials of gliomas, *Curr Oncol Rep* **12** no. 1 (2010) 68–75, http://dx.doi.org/10.1007/s11912-009-0078-3.
77. D. Wodarz, N. L. Komarova, *Computational Biology of Cancer: Lecture Notes and Mathematical Modeling.* World Scientific Publishing, Hackensack, NJ, 2005, http://dx.doi.org/10.1142/9789812701367

TRACHETTE L. JACKSON obtained her Ph.D. in applied mathematics from the University of Washington in 1998. The main focus of her research is combining mathematical modeling, numerical simulation, and *in vivo* tumor vascularization experiment to gain deeper understanding of tumor growth and vascular structure at the molecular, cellular, and tissue levels.
University of Michigan, Ann Arbor, MI 48109
tjacks@umich.edu

NATALIA L. KOMAROVA obtained her Ph.D. in applied mathematics from the University of Arizona in 1998. Her main interests are evolution, mathematical biology, and the mathematics of complex social phenomana. She co-authored more than 100 papers and four books.
University of California Irvine, Irvine CA 92697
komarova@uci.edu

KRISTIN R. SWANSON obtained her Ph.D. in applied mathematics from the University of Washington in 1999. Her research lab is focused on the practical application of patient-specific mathematical models for brain tumor growth to improve patient care. She is currently professor and vice chair of research in neurological surgery, professor in engineering sciences and applied mathematics, and director of the Mathematical Neuro-Oncology Lab at Northwestern University.
Northwestern University, Chicago, IL 60611
kristin.swanson@northwestern.edu

Author Proof